Correlation between morphology and defect luminescence in precipitated ZnO nanorod powders

ARTICLE *in* CRYSTAL GROWTH & DESIGN · FEBRUARY 2009

Impact Factor: 4.89

7 AUTHORS, INCLUDING:

Marko Bitenc
National Institute of Chemistry
12 PUBLICATIONS **192** CITATIONS

SEE PROFILE

Zorica Crnjak Orel
National Institute of Chemistry
124 PUBLICATIONS **1,423** CITATIONS

SEE PROFILE

Yuri Strzhemechny
Texas Christian University
75 PUBLICATIONS **1,196** CITATIONS

SEE PROFILE

Article

Correlation between Morphology and Defect Luminescence in Precipitated ZnO Nanorod Powders

Marko Bitenc, Peter Podbrs#c#ek, Zorica Crnjak Orel, Michael A. Cleveland, J. Antonio Paramo, Raul M. Peters, and Yuri M. Strzhemechny

Cryst. Growth Des., **2009**, 9 (2), 997-1001• DOI: 10.1021/cg8008078 • Publication Date (Web): 14 January 2009

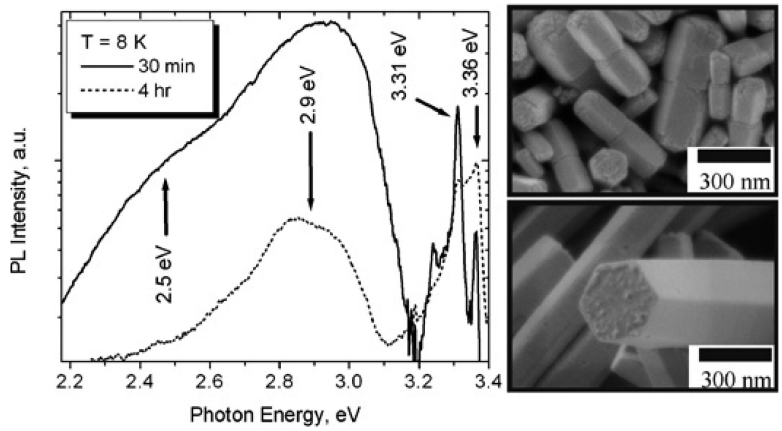

More About This Article

Additional resources and features associated with this article are available within the HTML version:

- Supporting Information
- Access to high resolution figures
- Links to articles and content related to this article
- Copyright permission to reproduce figures and/or text from this article

View the Full Text HTML

CRYSTAL GROWTH & DESIGN
2009
VOL. 9, NO. 2
997–1001

Correlation between Morphology and Defect Luminescence in Precipitated ZnO Nanorod Powders

Marko Bitenc,[†] Peter Podbršček,[†] Zorica Crnjak Orel,[†] Michael A. Cleveland,[‡] J. Antonio Paramo,[§] Raul M. Peters,[§] and Yuri M. Strzhemechny*[,§]

National Institute of Chemistry, 1000 Ljubljana, Slovenia, Physics Department, Austin College, Sherman, Texas 75090-4400, and Department of Physics and Astronomy, Texas Christian University, Fort Worth, Texas 76129

Received July 24, 2008; Revised Manuscript Received November 11, 2008

ABSTRACT: ZnO nanorods were prepared at relatively low temperatures by homogeneous precipitation from zinc nitrate and urea in a water/ethylene glycol mixture. Crystal size and morphology are controlled by growth time and solvent composition. We observed a strong correlation between nanocrystals' size/morphology and their optoelectronic defect-related properties. Smaller crystallites exhibited intense deep-defect luminescence and enhanced emission related to near-surface excitonic recombination. Longer growth times lead to formation of well-defined nanorods with hexagonal symmetry exhibiting reduced defect emission.

Introduction

Unique combination of valuable properties and hence numerous existing and potential applications of ZnO have attracted widespread attention in recent years. ZnO-based systems have already demonstrated excellent device performance in optoelectronics, sensors, acoustoelectrical and solar cell applications. The latest advances in crystal growth allowing production of high quality ZnO crystals render this material a good candidate for such applications as room temperature excitonic lasers, ultraviolet emitters and detectors, as well as high-temperature/high power microelectronics and spintronics.[1]

Remarkably, the area of ZnO-based nanostructures has developed into a significant, diverse, and rapidly expanding field.[1,2] The fact that the objects of interest are nanosize structures brings about distinct new phenomena. Moreover, since these ZnO nanostructures come in different sizes, shapes, and dimensionalities, each specific case of a nanostructure demonstrates its own set of properties. Thus, in the past few years numerous novel applications of nano-ZnO have been suggested and tested: LEDs photodetectors, field-effect transistors, bio- and chemical sensors, transducers, nanocantelivers, thermal transport elements, and so forth.

It is obvious that for many such applications, the ability to have an accurate control of the nanocrystal size and morphology is of fundamental importance. Existence of several control parameters within a straightforward and low-cost growth procedure should yield additional advantages.

Furthermore, the surface conditions of the nanostructures can play an exceptionally important role. In many instances of nanoscale applications for ZnO the quality of the surface and the subsurface layers is a key performance-defining parameter. By the same token, crystal surface could be a very significant source of lattice defects, as well as of contaminating impurities, and this influence may extend into the subsurface vicinity.[3,4] Hence, it is natural to expect that in nanocrystals, and in ZnO nanostructures in particular, surface-related defects may extend into the bulk of the material.[5] Moreover, the near-surface defect layer thickness may be comparable to the nanocrystal size. Hence, the contribution of defects should increase with the decreasing size of ZnO nanocrystals. Only in the past few years has it become clear that the current understanding of the surface properties of ZnO nanostructures and the ability to manipulate them are largely incomplete.[6−10] The nature of surface and subsurface defect states in nanosized ZnO is still ambiguous, and only in a small number of studies in the past few years were attempts made to tailor these states controllably.[11−15]

Recently, several reports were published addressing the relationship between the size of the ZnO nanostructures and their defect emission. However, these studies did not employ a consistent size-controlled growth of ZnO nanostructures with a well defined symmetry and/or morphology. For example, in refs 16−18 much smaller quantum-dot size objects were studied, revealing no specific symmetry or morphology. Alternatively, Shalish et al.[9] and Wang, et al.[19] were probing nano-objects within a certain size range from polydisperse nanonetworks. Attempts were also made to adjust particle sizes by applying different treatments[20] or by sampling relatively polydisperse nanopowders[21] obtained from different sources. In this paper we demonstrate for the first time that a low-temperature solution phase approach initially suggested in ref 22 can satisfy the requirements of a low-budget multiparameter controlled synthesis of high-quality hexagonal ZnO nanorods. Our results show that variation of the growth time, as well as the composition of the solvent, provides an accurate control of the size and morphology of the ZnO nanocrystals. Furthermore, we established a direct correlation between the morphology of the particles and their defect emission within a set of samples synthesized using a procedure with a consistent size-control.

Experimental Section

ZnO nano- and submicrometer sized rod-shaped structures were prepared by a homogeneous precipitation method at a relatively low temperature (90 °C) from zinc nitrate and urea in a water/ethylene glycol (W/EG) mixture. Fresh stock solutions were prepared from $Zn(NO_3)_2 \times 6H_2O$ (Aldrich) and urea (Aldrich) in MilliQue water. All reagents were analytically pure. The concentration of urea was kept constant at 0.05 mol dm^{-3} while the concentration of the Zn^{2+} ions was 0.01 mol dm^{-3}. The synthesis was performed employing continuous mixing in 250 mL open reactors. Different solvents were used: water and three W/EG mixtures with the volume ratios of 3/1, 1/1, and 1/3. Different growth times were applied. More detailed discussion of the growth procedure can be found in ref 22.

* To whom correspondence should be addressed. E-mail: y.strzhemechny@tcu.edu. Phone: (817) 257-5793. Fax: (817) 257-7742.
[†] National Institute of Chemistry.
[‡] Austin College.
[§] Texas Christian University.

10.1021/cg8008078 CCC: $40.75
Published on Web 01/14/2009

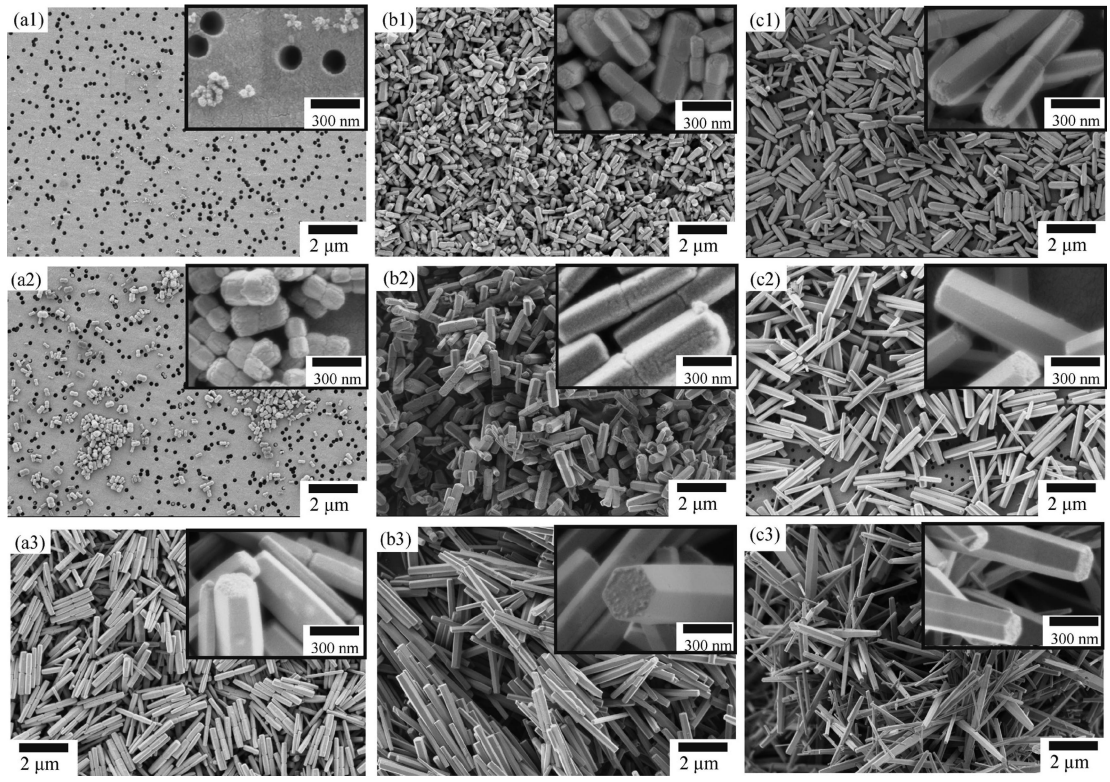

Figure 1. FE-SEM micrographs of the ZnO samples synthesized with different W/EG concentrations and for different times: (a1) W/EG 1/3, 30 min; (a2) W/EG 1/3, 45 min; (a3) W/EG 1/3, 4 h; (b1) W/EG 1/1, 30 min; (b2) W/EG 1/1, 45 min; (b3) W/EG 1/1, 4 h; (c1) W/EG 3/1, 30 min; (c2) W/EG 3/1, 45 min; (c3) W/EG 3/1, 4 h.

Morphology and structural properties of the synthesized samples were characterized by scanning field emission electron microscopy (SEM, Zeiss Supra 35 VP with an energy dispersive spectrometer) and X-ray diffraction (XRD) analysis, (Siemens D-500 X-ray diffractometer). Particle sizes and size distributions were determined from the SEM images using the CorelDraw software (100 nanocrystals were analyzed per sample). The infrared spectra were obtained on a Perkin-Elmer 2000 Fourier-transform infrared (FTIR) spectrometer in the spectral range between 4000 and 400 cm^{-1} with a spectral resolution of 2 cm^{-1} in the transmittance mode. The KBr pellets technique was used for sample preparation.

Optoelectronic characteristics were obtained using photoluminescence (PL) spectroscopy. The signal was excited by a CW Kimmon IK5452R-E HeCd laser with a wavelength of 325 nm. A variable frequency chopper was employed to provide a reference frequency. The samples were mounted inside an evacuated Janis CCS-150 cryostat having a temperature range between 8 and 325 K. The PL signal was probed by a Spex 1401 monochromator with a spectral resolution of 0.18 cm^{-1} and an RCA C31034 photomultiplier tube detector connected to a Stanford Research-830 lock-in amplifier for a background noise reduction.

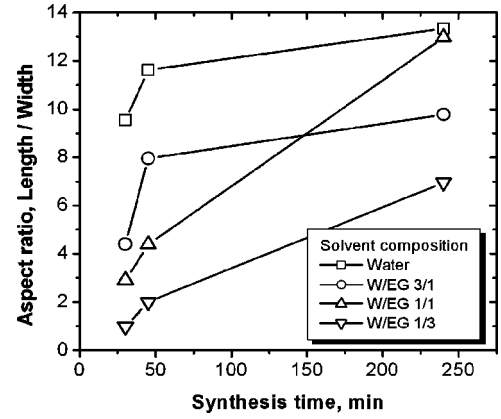

Figure 2. Length-to-width (L/W) aspect ratio of the ZnO nanorods obtained from the quantitative analysis of the SEM images (ca. 100 nanocrystals per sample were analyzed in CorelDraw).

Results and Discussion

Figure 1 shows SEM images of our samples for a range of different growth times and solvent compositions. One can observe a common trend: both the longitudinal and transverse average dimensions of the obtained hexagonal nanorods are increasing with the growth time, as well as with the water content in the solvent. CorelDraw-based quantitative analysis of the SEM images summarized in Figure 2 confirms such dependence of the growth dynamics (with an exception of a few outliers). Synthesis of similar ZnO nanorod networks was reported in a few recent publications,[23−25] for example, in ref. 23 where the authors employed a low-temperature seeded growth based on a zinc nitrate hydrate/hexamethylenetetramine solution to produce nanowire network transistors. However, practically no studies were reported on the growth parameters controlling dimensions and quality of the nanocrystals obtained. Our preparation approach provides well-defined size-controlling parameters.

For most of the samples reported here, the majority of the nanocrystals reveal transverse grooves close to the middle of the rod. At shorter growth times (and hence smaller rod sizes) this feature is more distinct, yielding an appearance of a dumbbell-shape bipod. Such feature was previously reported[26,27] and has been attributed to twinning mechanisms. In ref 27 it was suggested that ZnO nanostructures with dumbbell twinning may be used in applications for second harmonic generation in nonlinear optics.

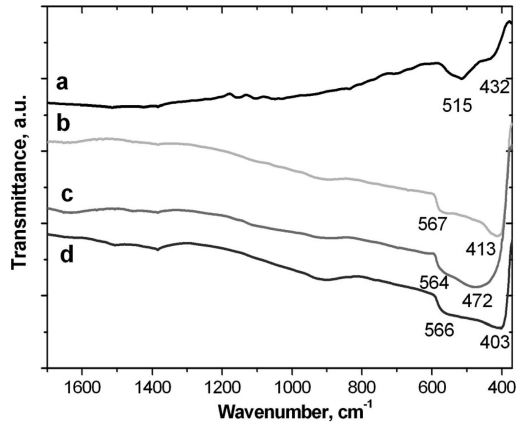

Figure 3. FTIR spectra of the ZnO nanorods synthesized in the W/EG 1/1 mixture for (a) 30 min, (b) 2 h, (c) 4 h, and (d) 24 h.

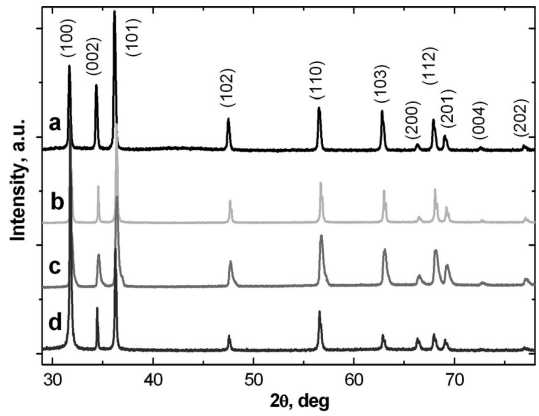

Figure 4. XRD spectra of the ZnO samples obtained after 4 h of synthesis employing different W/EG volume ratios: (a) water only, (b) 3/1, (c) 1/1, and (d) 1/3.

FTIR spectra of the samples prepared in a W/EG solution for 0.5, 2, 4, and 24 h are presented in Figure 3. All the spectra show the Zn−O stretching bands in the 600 to 400 cm^{-1} range confirming formation of ZnO within this synthesis time. The relative intensity of these features as a function of the growth time is rather consistent with the nanocrystal sizes as derived from the SEM results. FTIR spectra of the 600−400 cm^{-1} characteristic range can be used not only for a qualitative analysis but also as confirmation of the shape of the ZnO particles.[22,28,29]

XRD spectra of the samples grown for 4 h in water and in the W/EG media with the volume ratios of 1/3, 1/1, and 3/1 are presented in Figure 4. All the major spectral features correspond to the ZnO reflections, as indicated in the graph. Very similar XRD spectra were also obtained for the samples prepared in other W/EG mixtures and within all growth times (not shown). The quality of the synthesized nanocrystalline structures, as judged by the peak widths and peak positions, is rather uniform. Sample-to-sample difference in the relative intensities of the XRD features is most likely associated with the variation of the orientational texture of the grown nanorod networks, consistent with the SEM images.

Thus, our measurements indicate that the suggested wet solution-phase approach provides an inexpensive and effective routine for growing well-defined hexagonal ZnO nanorods with an accurate control of the nanocrystal length and thickness through synthesis time and solvent contents. Discussion of the possible underlying mechanisms of such dependence on the time and chemistry is provided in ref 22.

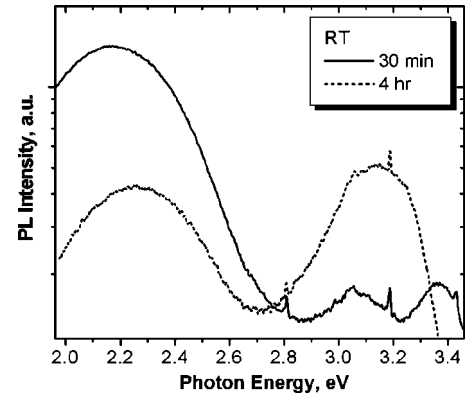

Figure 5. Comparison between room temperature PL spectra of the samples obtained after 30 min and 4 h of synthesis in the W/EG 1/1 mixture.

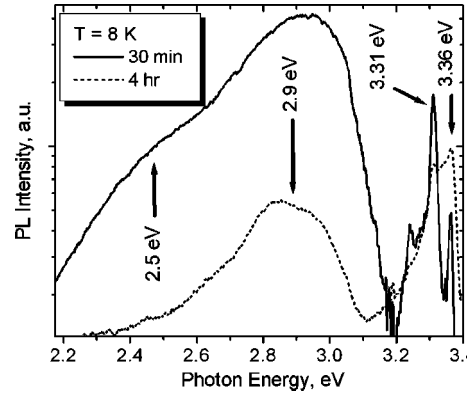

Figure 6. Comparison between low temperature (8 K) PL spectra of the samples obtained after 30 min and 4 h of synthesis in the W/EG 1/1 mixture.

We employed PL measurements to verify how the morphology of our samples affects their optoelectronic characteristics. Such relationship has been investigated in recent years for a number of different ZnO nanosystems.[9,16−21] The most fundamental question arising in this regard is whether the substantially increased surface to volume ratio in a nanosystem leads to a significant rearrangement of defect-related radiative and nonradiative recombinations. Various surface-related mechanisms affecting luminescence properties of nanosize ZnO crystals were suggested: significant contribution of a surface-defect-bound exciton emission,[7,8,10,21,30−34] near-surface recombination mediated by the depletion layer,[9,35,36] existence of a defect-rich subsurface layer,[5] and so forth. Our growth procedure provided consistent sampling of ZnO nanostrutures to address the issue of size-scaling of defect luminescence. In our samples we observed a strong correlation between their morphology and defect properties as illustrated by Figures 5−7.

Figure 5 shows a comparison between room temperature PL spectra of the 30 min and 4 h nanorod samples. The 30 min samples reveal a very intense deep defect emission at ∼2.2 eV. The deep level defects are most likely oxygen deficiency-related.[36] One can also see two relatively weak near-band gap emission broad peaks at 3.15 and 3.35 eV. On the other hand, for the longer growth times, the relative intensity of the deep defect luminescence is lower by an order of magnitude. The presence of two features near-band gap features was observed

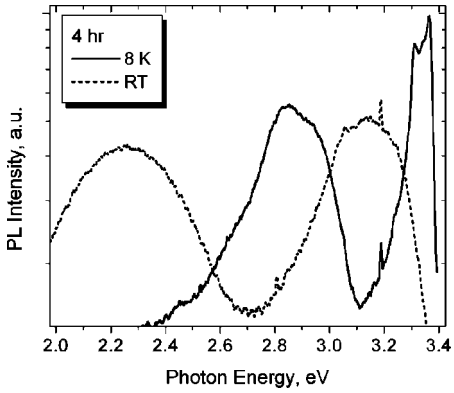

Figure 7. Comparison between low temperature (8 K) and room temperature PL spectra of the ZnO nanorod samples obtained after 4 h of synthesis in the W/EG 1/1 mixture.

only in the 30 min samples and requires further elucidation. Insignificant spectral differences between the 4 and 24 h growth times (not shown) are consistent with the morphological similarity of these specimens as detected by the SEM. The results of Figure 5 can be explained within the assumption that in smaller crystals the relative radiative contribution of the deep defect-rich near-surface layers is substantially greater.

Figure 6 juxtaposes low temperature (8 K) PL spectra of the 30 min and 4 h samples. The following features appear in the spectra: sharp excitonic emissions at $\sim$ 3.31 eV and $\sim$ 3.36 eV, a "blue-violet" recombination at $\sim$ 2.9 eV due to relatively shallow defects, and a "green" deep defect band at $\sim$2.5 eV. In a recent paper,[21] the 3.31 eV peak was attributed to a surface defect-related excitonic luminescence. Accepting this assignment one can see that in smaller (30 min) crystallites, the relative intensity of this emission is much stronger compared to the one in the well defined nanorods. Thus, for smaller morphologies, the surface defect layer is likely to become predominant. Also, the relative intensity of the deep-defect ("green") and shallower-defect ("blue-violet") emission is higher by an order of magnitude in the 30 min samples, indicating an elevated contribution from the deep and shallower defects compatible with a greater volume fraction of the defective near-surface layer.

There also exists a significant temperature-mediated rearrangement of recombination channels in our ZnO nanorods as can be seen from Figure 7, which contrasts the low temperature and room temperature PL spectra of the long nanorod samples. The defect-related recombination is dominated at room temperature by the green emission (probably related to oxygen deficiency), whereas in the low-temperature spectra the green emission is suppressed by the blue-violet luminescence, suggesting the existence of competing recombination centers. Such competition in bulk ZnO was described previously,[37] and the nature of the shallow centers still remains disputable.

Conclusions

We established a growth procedure for ZnO quasi-1D nanostructures allowing good control of their size, which in turn affects the defect properties of the material. Both the growth time and the solvent composition determine morphology and quality of the samples. Shorter growth times result in smaller particles with rougher surfaces, lesser morphological anisotropy, and conspicuous mid-rod bipod twining. Longer growth times yield well defined nanorods with distinct hexagonal symmetry. We observed a strong correlation between the morphology of our samples and their defect luminescent properties, confirming a hypothesis that the radiative contribution of defects should increase with the decreasing nanocrystal size.

Acknowledgment. This work is supported by the Ministry of Higher Education, Science and Technology of the Republic of Slovenia, and the Slovenian Research Agency (program P1-0030, project J2-6027), NSF REU Grant (PHYS-0453577) and the TCU RCAF Grant (# 60535). The authors would also like to thank W. Pagdon (Jobin Yvon) for fruitful technical discussions.

References

(1) Özgür, Ü.; Alivov, Ya. I.; Liu, C.; Teke, A.; Reshchikov, M. A.; Doan, S.; Avrutin, V.; Cho, S.-J.; Morkoc, H. *J. Appl. Phys.* **2005**, *98*, 041301; and references therein.
(2) Wang, Z. L. *J. Phys.: Condens. Matter* **2004**, *16*, R829; and references therein.
(3) Mosbacker, H. L.; Strzhemechny, Y. M.; White, B. D.; Smith, P. E.; Look, D. C.; Reynolds, D. C.; Litton, C. W.; Brillson, L. J. *Appl. Phys. Lett.* **2005**, *87*, 012102.
(4) Strzhemechny, Y. M. *J. Vac. Sci. Technol. A* **2006**, *24*, 1233.
(5) Fischer, A. M.; Srinivasan, S.; Garcia, R.; Ponce, F. A.; Guaño, S. E.; Di Lello, B. C.; Moura, F. J.; Solórzano, I. G. *Appl. Phys. Lett.* **2007**, *91*, 121905.
(6) Hirai, T.; Harada, Y.; Hashimoto, S.; Ohno, N.; Itoh, T. *J. Lumin.* **2005**, *113*, 115–120.
(7) Grabowska, J.; Nanda, K. K.; McGlynn, E.; Mosnier, J.-P.; Henry, M. O.; Beaucamp, A.; Meaney, A. *J. Mater. Sci.: Mater. Electron.* **2005**, *16*, 397–401.
(8) Grabowska, J.; Meaney, A.; Nanda, K. K.; Mosnier, J.-P.; Henry, M. O.; Duclère, J.-R.; McGlynn, E. *Phys. Rev. B* **2005**, *71*, 115439.
(9) Shalish, I.; Temkin, H.; Narayanamurti, V. *Phys. Rev. B* **2004**, *69*, 245401.
(10) Wischmeier, L.; Voss, T.; Börner, S.; Schade, W. *Appl. Phys. A: Mater. Sci. Process.* **2006**, *84*, 111–116.
(11) Sakohara, S.; Ishida, M.; Anderson, M. A. *J. Phys. Chem. B* **1998**, *102*, 10169–10175.
(12) Guo, L.; Yang, S.; Yang, C.; Yu, P.; Wang, J.; Ge, W.; Wong, G. K. L. *Appl. Phys. Lett.* **2000**, *76*, 2901–2903.
(13) Li, J.; Zhao, D.; Meng, X.; Zhang, Z.; Zhang, J.; Shen, D.; Lu, Y.; Fan, X. *J. Phys. Chem. B* **2006**, *110*, 14685–14687.
(14) Yang, Y.; Tay, B. K.; Sun, X. W.; Sze, J. Y.; Han, Z. J.; Wang, J. X.; Zhang, X. H.; Li, Y. B.; Zhang, S. *Appl. Phys. Lett.* **2007**, *91*, 071921.
(15) Yang, Y.; Sun, X. W.; Tay, B. K.; Cao, P. H. T.; Wang, J. X.; Zhang, X. H. *J. Appl. Phys.* **2008**, *103*, 064307.
(16) van Dijken, A.; Meulenkamp, E. A.; Vanmaekelbergh, D.; Meijerink, A. *J. Lumin.* **2000**, *87*−*89*, 454–456.
(17) van Dijken, A.; Makkinje, J.; Meijerink, A. *J. Lumin.* **2001**, *92*, 323–328.
(18) Li, J. F.; Yao, L. Z.; Ye, C. H.; Mo, C. M.; Cai, W. L.; Zhang, Y.; Zhang, L. D. *J. Cryst. Growth* **2001**, *223*, 535–538.
(19) Wang, Y. W.; Zhang, L. D.; Wang, G. Z.; Peng, X. S.; Chu, Z. Q.; Liang, C. H. *J. Cryst. Growth* **2002**, *234*, 171–175.
(20) Huang, M. H.; Wu, Y.; Feick, H.; Tran, N.; Weber, E.; Yang, P. *Adv. Mater.* **2001**, *13*, 113–116.
(21) Fallert, J.; Hauschild, R.; Stelzl, F.; Urban, A.; Wissinger, M.; Zhou, H.; Klingshirn, C.; Kalt, H. *J. Appl. Phys.* **2007**, *101*, 073506.
(22) Bitenc, M.; Crnjak Orel, Z. *Mater. Res. Bull.* [Online early access]. DOI: 10.1016/j.materresbull.2008.05.005. Published online: **2008**.
(23) Ko, S. H.; Park, I.; Pan, H.; Misra, N.; Rogers, M. S.; Grigoropoulos, C. P.; Pisano, A. P. *Appl. Phys. Lett.* **2008**, *92*, 154102.
(24) Clavel, G.; Willinger, M.-G.; Zitoun, D.; Pinna, N. *Adv. Funct. Mater.* **2007**, *17*, 3159–3169.
(25) Buha, J.; Djerdj, I.; Niederberger, M. *Cryst. Growth Des.* **2007**, *7*, 113–116.
(26) Wang, B. G.; Shi, E. W.; Zhong, W. Z. *Cryst. Res. Technol.* **1998**, *33*, 937–941.
(27) Liu, S. W.; Zhou, H. J.; Ricca, A.; Tian, R.; Xiao, M. *Phys. Rev. B* **2008**, *77*, 113311.
(28) Hayashi, S.; Nakamori, N.; Kanamori, H. *J. Phys. Soc. Jpn.* **1979**, *46*, 176–183.

(29) Verges, A. M.; Mifsud, A.; Serna, C. J. *J. Chem. Soc., Faraday Trans.* **1990**, *86*, 959–963.
(30) Travnikov, V. V.; Freiberg, A.; Savikhin, S. F. *J. Lumin.* **1990**, *47*, 107–112.
(31) Hirai, T.; Harada, Y.; Hashimoto, S.; Ohno, N.; Itoh, T. *J. Lumin.* **2005**, *112*, 196–199.
(32) Wischmeier, L.; Voss, T.; Rückmann, I.; Gutowski, J.; Mofor, A. C.; Bakin, A.; Waag, A. *Phys. Rev. B* **2006**, *74*, 195333.
(33) Voss, T.; Bekeny, C.; Wischmeier, L.; Gafsi, H.; Börner, S.; Schade, W.; Mofor, A. C.; Bakin, A.; Waag, A. *Appl. Phys. Lett.* **2006**, *89*, 182107.
(34) Stichtenoth, D.; Ronning, C.; Niermann, T.; Wischmeier, L.; Voss, T.; Chien, C.-J.; Chang, P.-C.; Lu, J. G.*Nanotechnology* **2007**, *18*, 435701.
(35) Vanheusden, K.; Seager, C. H.; Warren, W. L.; Tallant, D. R.; Voigt, J. A. *Appl. Phys. Lett.* **1996**, *68*, 403–405.
(36) Vanheusden, K.; Warren, W. L.; Seager, C. H.; Tallant, D. R.; Voigt, J. A.; Gnade, B. E. *J. Appl. Phys.* **1996**, *79*, 7983–7990.
(37) Strzhemechny, Y. M.; Nemergut, J.; Smith, P. A.; Bae, J.; Look, D. C.; Brillson, L. J. *J. Appl. Phys.* **2003**, *94*, 4256.

CG8008078